

1           **NEOFORMED MINERAL PHASES DURING CLAY CERAMIC FIRING**

2 M. EL OUAHABI<sup>1\*</sup>, L. DAOUDI<sup>2</sup>, F. HATERT<sup>3</sup> AND N. FAGEL<sup>1</sup>,

3 <sup>1</sup> UR Argile, Géochimie et Environnement sédimentaires (AGEs), Département de Géologie  
4 B-18, Sart-Tilman, Université de Liège, Liège, B-4000, Belgium.

5 <sup>2</sup> Laboratoire de Géosciences et Environnement, Département de Géologie, Faculté des  
6 Sciences et Techniques, BP 549, Marrakech, Morocco.

7 <sup>3</sup> Laboratory of Mineralogy, B-18, University of Liège, B-4000, Liège, Belgium.

8

9

10

11

12

13

14

15

16 \*Corresponding author: Département de Géologie, Sart-Tilman B18, Allée du 6 Août, B-4000  
17 Liège, Belgium

18 Tel: +32. (0)4. 366.2210; Fax: +32. (0)4.366.2029

19 E-mail address: Meriam.ElOuahabi@ulg.ac.be

20

21

22

23

24

25

26        **ABSTRACT**

27        Ceramic clays are one of the most complicated ceramic systems because of the very complex  
28        relationship between the behavior of minerals during the ceramic processing and the  
29        transformations during heating. A major challenge is to predict the phase transformations in  
30        clay ceramics. The aims are to establish reference data of ceramics products that can be  
31        formed based on the mineralogical composition of the local raw materials. These data, in turn,  
32        can be compared with the archaeological ceramics in order to study their origins.

33        The mineralogical compositions and transformations during the firing (550 to 1100°C under  
34        oxidizing conditions) of seven clayey materials sampled from the main clay deposits of  
35        Northern Morocco were evaluated by X-ray powder diffraction. Two groups of clays were  
36        evidenced according to the type of neoformed high-temperature minerals: non-calcareous  
37        clays and calcareous clays. For the non-calcareous raw materials, spinel is produced at 950°C.  
38        Cristobalite and mullite were formed above 1000°C from clays that contain illite, kaolinite  
39        and chlorite. In clays containing vermiculite and high amount of chlorite, hematite was  
40        formed from 950°C. Firing of calcareous clays at temperatures > 950°C yielded Ca-silicates  
41        (diopside, gehlenite and wollastonite), spinel, cristobalite, hematite and feldspars. Mullite may  
42        also form in the calcareous clay products, when the carbonates content exceeds 10%.

43

44

45        *Keywords:* Clay; Raw materials; Ceramic; X-ray powder diffraction; Neof ormation

46

47

48

49 **INTRODUCTION**

50 Clay minerals undergo a complex path of thermal transformations during heating (Henn *et*  
51 *al.*, 2007; Kam *et al.*, 2009), which determine the final properties of the ceramic products. A  
52 major challenge is to predict the phase transformations in fired ceramic clays, since complex  
53 relationships occur between the structural characteristics of the fired products and the  
54 chemical properties of the fired ceramics.

55 Upon firing, the minerals in the fired ceramic clays undergo chemical and structural  
56 modifications deeply transforming the original clayey materials. The high temperature, low-  
57 pressure mineral transformations are mainly influenced by the chemical and mineralogical  
58 compositions of the raw materials, the maximum heating temperature, heating rate, duration  
59 of firing and kiln redox atmosphere (Lin, 2007; Khalfaoui and Hajjaji, 2009; Pardo *et al.*,  
60 2011).

61 Fired ceramic clays have a complex mineralogical composition, which makes the study of  
62 neomineralizations and the disappearance of mineral phases present in the raw material rather  
63 difficult (Jordán *et al.*, 2001). It is difficult to maintain the stability of these crystalline  
64 structures, once they cross their stability limits, partially decompose and then simultaneously  
65 form other phases (Jordán *et al.*, 1999).

66 The present work focuses on the mineral transformations with increasing temperature for 7  
67 clays of widely varying mineralogies from northern Morocco to assess their suitability for the  
68 production of ceramics. The main aim was to study the mineral transformations of natural  
69 clays with increasing temperature and to establish reference groups for local ceramic industry  
70 based on raw-material composition and high-temperature mineralogy.

Code de champ modifié

Code de champ modifié

Code de champ modifié

Code de champ modifié

Code de champ modifié

Code de champ modifié

71 **MATERIALS AND METHODS**

72 The studied clays belong to three clay deposits of Morocco which can be used in ceramic  
73 pastes. The clays came from Northern Morocco at Meknes, Tangier and Tetouan regions. The  
74 geological background of the mineralogical, textural, and geotechnical compositions of those  
75 clays were previously described by El Ouahabi *et al.* (2014b).

Code de champ modifié

76 Seven samples have been selected based on the mineralogical characterization of 52 clay  
77 samples from the main clay deposits of Northern Morocco (El Ouahabi *et al.*, 2014b). The  
78 samples representing the observed compositional variability were selected for firing  
79 experiments to study the mineral evolution during ceramic firing process. The main  
80 compositional criteria were related to the presence/absence of carbonates, their composition  
81 (calcite or dolomite) and abundance, the type of phyllosilicates (clay minerals) and their  
82 relative proportions, and the presence/absence of Fe-rich minerals (hematite). Following their  
83 mineralogical composition, we identified two groups of clays, rich in carbonates (CC) and  
84 non-calcareous (NC) clays. The presence of carbonates, as well as their type (calcite or  
85 dolomite) affects the firing behavior and crystallization of minerals at high temperatures (Tite  
86 and Maniatis, 1975; Czimerová *et al.*, 2006; Demir, 2008).

Code de champ modifié

Code de champ modifié

Code de champ modifié

87 The studied clays were composed mostly of quartz, illite, kaolinite and variable amounts of  
88 calcite, chlorite, vermiculite, smectite, feldspars, hematite and muscovite (El Ouahabi *et al.*,  
89 2014b). The chemical composition (Table 1) of the selected clays consist of SiO<sub>2</sub> (35 - 51%),  
90 Al<sub>2</sub>O<sub>3</sub> (14 – 34%), CaO (0 – 19%), Fe<sub>2</sub>O<sub>3</sub> (0 – 15%), and small amount of MgO and K<sub>2</sub>O (El  
91 Ouahabi *et al.*, 2014a).

Code de champ modifié

Code de champ modifié

92 Seven clay samples were oven dried at 35°C for 48 h. Dried clay was ground and sieved  
93 through 20 mm to simulate industrial pressing conditions. Each clay sample was wetted in

94 order to achieve the proper plasticity for molding. The samples obtained with these shaping  
95 techniques were: 4 cm long, 2 cm wide and 2 cm thick. The drying was done in shaded and  
96 ventilated room. The dried samples (24 h at shaded room plus 12 h at 105°C in oven) were  
97 kiln-fired at different temperatures (550, 950, 1000 and 1100°C) for 1h at rate of 10°C/min.  
98 The analysis of mineralogical phases of the fired samples was carried out by X-ray diffraction  
99 (XRD), using Bruker D8-Advance diffractometer with CuK $\alpha$  radiations (Department of  
100 Geology, University of Liege, Belgium) on powdered bulk sediment following the procedure  
101 for clay analysis, as described by Trindade *et al.* (2009). The X-ray powder patterns were  
102 treated by the DIFFRACplus EVA software to remove the background noise and to calculate  
103 profile parameters such as line positions and peak intensities. The estimation of mineralogical  
104 composition is based on the maximum count rate at the top of each characteristic peak d(001).

Code de champ modifié

105 The chemical composition of selected elements (Si, Al, Fe, Ca, Mn, Mg, Na, K, Ti, P and S)  
106 was measured as oxides on 2 g of dried and homogenized powder of clayey samples using a  
107 Bruker S8 Tiger wavelength-dispersive X-Ray Fluorescence (WD-XRF) spectrometer  
108 equipped with a Rh anticathode (Department of Ecology and Environmental Sciences, Umeå  
109 University, Sweden). Reproducibilities are above 99% except for S (89%) and P (97%). More  
110 details about the method and the calibration can be found in De Vleeschouwer *et al.*, (2011).  
111 The same powdered samples were heated to 1000°C for 2 h to determine the Loss On Ignition  
112 (L.O.I).

Code de champ modifié

## 113 **RESULTS AND DISCUSSION**

114 The clay ceramic industries are usually based on chemical data (XRF) to predict the  
115 neoformation of crystalline phases during firing. The implication of carbonates and non-  
116 calcareous clays in the formation of the glassy phase, mullite, and cristobalite is discussed by  
117 using SiO<sub>2</sub>/Al<sub>2</sub>O<sub>3</sub>/NaO<sub>2</sub>+K<sub>2</sub>O and SiO<sub>2</sub>/Al<sub>2</sub>O<sub>3</sub>/CaO equilibrium diagrams (Figure 1).

118 Due to the position of the representative points of the chemical compositions of original  
119 phases  $\text{SiO}_2/\text{Al}_2\text{O}_3/\text{NaO}_2+\text{K}_2\text{O}$  diagram (Figure 1), mullite should be formed. Referring to  
120 literature data (Cultrone *et al.*, 2001; Khalfaoui and Hajjaji, 2009), mullite is derived from the  
121 aluminum content, related to the presence of clay minerals and micaceous-rich minerals.

Code de champ modifié

Code de champ modifié

122 In the  $\text{SiO}_2/\text{Al}_2\text{O}_3/\text{CaO}$  equilibrium diagram (Levin *et al.*, 1964), non-calcareous materials  
123 produce high temperature phases such as mullite. In the calcareous clays the presence of CaO  
124 avoid the formation of the mullite. Decomposed clay minerals form, in combination with  
125 CaO, phases like gehlenite, anorthite, wollastonite, instead of mullite (Peters and Iberg, 1978;  
126 Czímerová *et al.*, 2006). For the silica-rich, material cristobalite phase was formed in  
127 carbonate-rich clays. Tridymite could also be observed as an intermediate phase before the  
128 formation of the cristobalite, depending on the relative proportions of the three components  
129 ( $\text{SiO}_2$ ,  $\text{Al}_2\text{O}_3$ , CaO) and the temperature of firing.

130 The results (Figure 2 and 3a-b) and related discussion for mineralogical transformations as  
131 function of temperature are based on the two groups of raw materials defined above: (1) non-  
132 calcareous clays; (2) and carbonate rich clays. The mineral abbreviations used in this study  
133 are from Whitney and Evans (2010).

134 Overall, the first mineral transformations (Figures 2a-b and 3) observed with increasing  
135 temperature included the dehydroxylation of kaolinite before  $550^\circ\text{C}$ , followed by other clay  
136 minerals (illite, chlorite, smectite, and vermiculite), which dehydroxylated close to  $950^\circ\text{C}$ .  
137 Calcite and dolomite transformed into lime (CaO) and then reacted with other components to  
138 generate neofomed calcium minerals, such as gehlenite, diopside and wollastonite (Trindade  
139 *et al.*, 2009). Generally, K-feldspars disappeared below  $1000^\circ\text{C}$ , plagioclase seemed to persist  
140 up to  $1100^\circ\text{C}$ , and quartz is preserved even at  $1100^\circ\text{C}$ .

141 **Non-calcareous clays**

142 Three non-calcareous clay samples (NC1, NC2 and NC3) were kaolinitic and illitic clays  
143 with high quartz content (Figure3 and 4a). Chlorite was only present in NC2 and NC3 in  
144 small amount. Smectite was present in NC1 (El Ouahabi *et al.*, 2014b). Small amount of  
145 hematite was observed. Plagioclase was another constituent, which was absent in NC3 clay.

Code de champ modifié

146 Relative to mineral transformations (Figures 3a, 4a, and 5) of NC1, kaolinite and  
147 illite/smectite disappeared at 550°C and 950°C, respectively. Plagioclase and muscovite  
148 disappeared close to 950°C and was replaced by alkali feldspars. Quartz and hematite were  
149 present throughout the entire temperature range. Hematite showed a slight increase, whereas  
150 quartz is reduced by a factor of 2 at the maximum firing temperature. Neofomed mullite and  
151 K-feldspar appeared at 950°C and reached its maximum abundance at 1100°C.

152 Despite their variable starting composition, NC2 and NC3 showed similar neofomed  
153 minerals. Mineral transformations with firing included the loss of all phyllosilicates from 950  
154 to 1000°C, muscovite at 950°C, and plagioclase close to 1100°C. Quartz and hematite  
155 remained up to 1100°C, with their maximum abundance at maximum fired temperature.  
156 Spinel formed at 950°C, followed by mullite and cristobalite at 1000°C. Mullite and  
157 cristobalite were more abundant at 1100°C.

158 All the samples studied contain Mg-rich spinel, probably derived from the dehydroxylation  
159 of clay minerals rich in MgO, chlorite and smectite. Spinel was formed by the reaction:  $MgO$   
160  $+ Al_2O_3 \rightarrow MgAl_2O_4$ . Cristobalite and mullite are found in NC2 and CN3, due to  
161 phyllosilicates transformation, particularly illite (Cultrone *et al.*, 2001). According to their  
162 mineralogical composition, those clays contain ~20% of muscovite and illite, respectively (El  
163 Ouahabi *et al.*, 2014b). Cristobalite is probably produced by quartz transformation, as

Code de champ modifié

Code de champ modifié

164 observed previously (e.g., Elert *et al.*, 2003). The major original mineral at high-temperature  
165 is quartz, which is the most abundant phase in all fired clay samples. Other original minerals  
166 accompanying quartz up to 1100°C are hematite.

Code de champ modifié

167 The neoformed mineralogy for non-calcareous clays was relatively simple, consisting of  
168 spinel, cristobalite, and mullite and K-feldspar. Mullite appeared at 1000°C in quartz rich  
169 clays, and its abundance increased at higher temperatures (Figure 5). One could say that the  
170 quartz content (about 50%) in addition to phyllosilicates promote the formation of mullite.  
171 Cristobalite was identified only in the quartz-rich clays (NC2 and NC3) at 1000°C. The  
172 neoformed K-feldspar observed after firing at high temperatures in NC1 clay is suggested to  
173 be a high-temperature phase which replaced illite/muscovite phase.

174 Firing below 950°C induced no significant mineralogical transformations and  
175 neoformations began from 950°C. Feldspars (K-feldspar and plagioclase) neoformed at  
176 950°C, act as a flux that facilitate easy melting at firing. During clay firing especially,  
177 micaceous minerals especially change to mullite, K-feldspar and plagioclase (Cultrone *et al.*,  
178 2001; Khalfaoui and Hajjaji, 2009).

Code de champ modifié

Code de champ modifié

### 179 **Carbonate rich clays**

180 Four carbonate rich clays (CC1-CC4) were kaolinitic and illitic clays (Figures 3b, 4b and  
181 5), with a high quartz content. Chlorite is the major clay mineral phase in the CC1 sample,  
182 while it is found in trace amounts in the other samples. In CC3 sample, vermiculite is the  
183 principal clay mineral phase. Variable amounts of calcite were identified, whereas small  
184 amounts of dolomite, plagioclase and K-feldspar are present in these carbonate clays (El  
185 Ouahabi *et al.*, 2014a).

Code de champ modifié



186 For CC1, calcite, phyllosilicates were the first minerals to disappear at 950°C. Plagioclase,  
187 dolomite and quartz were present throughout the temperature range, but the abundance of  
188 quartz and dolomite decreased at 1100°C. The first minerals neoformed were gehlenite and  
189 diopside, which appeared at 950°C, followed by spinel at 1000°C. The gehlenite content  
190 decreased at higher temperatures, and diopside and spinel were more abundant at 1100°C. K-  
191 feldspar disappeared close to 950°C, plagioclase seemed to persist up to 1100°C, and  
192 increased in amount.

193 The mineralogical transformations, reported in figures 2b and 3b, indicate that when the  
194 temperature is increased to 950°C,  $\text{CaCO}_3$  decomposes to CaO, phyllosilicates decompose  
195 and spinel type phases appear. CaO reacts with Si and Ca-silicates appear, such as gehlenite,  
196 diopside and wollastonite. As the temperature further increases, the gehlenite content  
197 decreases; this mineral seems to be a metastable neoformed phase.

198 The first mineralogical transformations of CC2 were the disappearance of calcite,  
199 phyllosilicates at 950°C. Plagioclase, K-feldspar, dolomite and quartz were still abundant after  
200 firing at 1100°C. Plagioclase and K-feldspar increased their abundance up to 1000°C.  
201 Gehlenite, diopside and hematite were first neoformed minerals identified at 950°C, and their  
202 abundance was maximum at 1100°C. Hematite resulted from the iron released during chlorite  
203 and illite decomposition. Spinel and cristobalite were present at 1000°C; their maximum  
204 abundance was observed at 1100°C. Mullite was the last phase neoformed at high  
205 temperature, close to 1100°C.

206 Relative to mineral transformations of CC3, kaolinite disappeared at 550°C, whereas  
207 calcite and vermiculite were persisted up to 950°C. Quartz was the only one present  
208 throughout the entire temperature range, with its abundance being very low at the maximum  
209 firing temperature. Neoformed minerals were diversified; they included plagioclase, K-

210 feldspar, diopside, gehlenite and hematite. All neoformed minerals appeared at 950°C and  
211 were most abundant at 1100°C, with an exception for hematite and gehlenite.

212 During firing of CC4, phyllosilicates disappeared at 950°C and K-feldspar at 1000°C.  
213 Plagioclase and quartz remained at the highest temperature of firing in very small amounts.  
214 Gehlenite, diopside, cristobalite and spinel formed at 950°C, where they attained maximum  
215 abundance at 1000°C. Later, wollastonite is formed at 1100°C, with relatively high  
216 abundance. Diopside, cristobalite, gehlenite and spinel increase their abundance gradually.

217 The most significant mineralogical changes are observed in samples with carbonates, when  
218 fired at  $T > 800^{\circ}\text{C}$ . Firing caused the decomposition of carbonates, clay minerals, and silicates  
219 and the formation of a melt phase rich in Si, Al, Ca, and K (Czímerová *et al.*, 2006). From this  
220 melt phase, neoformation and crystallization of several metastable phases occurred,  
221 continuously reacting with increasing temperature.

Code de champ modifié

222 All the calcareous clay samples contain gehlenite and diopside, which formed due to the  
223 presence of  $\text{CaCO}_3$ . In addition hematite, spinel, cristobalite and anorthite are formed.  
224 Wollastonite is neoformed only in CC4 at high temperature close to 1100°C. Melting starts  
225 just before 950°C when carbonates are present (Tite and Maniatis, 1975). Ca and Mg from  
226 carbonates may act as melting agents but they are reported to somehow limit the extent of  
227 vitrification at temperature above 1000°C (Cultrone *et al.*, 2001). On the other hand, the  
228 higher  $\text{SiO}_2$  content in these samples provides a higher amount of potential silica-rich melt.

Code de champ modifié

Code de champ modifié

229 Gehlenite starts to form between 550 and 950°C, when Mg is absent, by reaction between  
230 CaO from carbonates,  $\text{Al}_2\text{O}_3$  and  $\text{SiO}_2$  from the dehydroxylated phyllosilicates (Peters and  
231 Iberg, 1978). Diopside starts also to form between 550 and 950°C in all calcareous clays by  
232 reacting of Ca, Mg and  $\text{SiO}_2$  from dolomite and quartz for CC1 and CC2; however Ca is

Code de champ modifié

233 probably supplied from calcite, Mg seem to come from vermiculite or chlorite for CC3 and  
234 CC4. In the case of wollastonite, these mineral stemmed from reaction of CaO with SiO<sub>2</sub> at high  
235 temperature, its neoformation is marked mainly by a sharp decrease in quartz content (Figure  
236 5). Wollastonite improves strength as well as water and heat resistances of ceramics (Azarov  
237 *et al.*, 1995).

Code de champ modifié

238 Neoformed hematite resulted from dehydroxylation of Fe-rich clay such as vermiculite, in  
239 our case. Unfired clays with hematite, increased their amount in heated samples with rising  
240 temperature. This suggests that ferric oxide may be formed by the decomposition of clay  
241 minerals with non-negligible amounts of iron (Murad and Wagner, 1998). At higher  
242 temperature (1100°C) phyllosilicates have already disappeared in all samples, being  
243 transformed into spinel for most of clays, and further into mullite for CC2. Thus, the spinel  
244 phase essentially originated from decomposed chlorite, i.e. the principal Mg-bearing mineral.  
245 Spinel is absent in clays that do not contain chlorite (CC3). Between 550 and 950°C, the  
246 appearance of the reflections at 3.2 Å, 3.18 Å and 4.4 Å for CC3 indicated the formation of  
247 calcium aluminium silicate phase, anorthite (CaAl<sub>2</sub>Si<sub>2</sub>O<sub>8</sub>).

Code de champ modifié

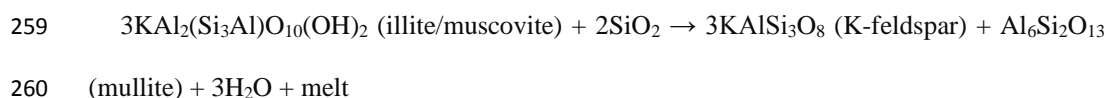
248 The most significant difference between the calcareous fired clays is the appearance of  
249 mullite and hematite only in CC2 from 1000 and 550°C, respectively. Mullite appeared at  
250 high temperature, which could be related to the presence of enough content of  
251 illite/muscovite. At 1100°C, when illite and muscovite have already disappeared. They react  
252 with quartz, being transformed into mullite plus a melt (Cultrone *et al.*, 2001). During firing,  
253 Fe is generally responsible for the formation of mullite (Cuevas *et al.*, 2009). Plagioclase  
254 decreases slowly and K-feldspar decreased at 1000°C. Feldspars (especially alkali feldspars)  
255 are fluxes, so they may be neoformed during firing, as demonstrated by their increase from  
256 1000°C, which can be attributed to the formation of mullite (Czimerová *et al.*, 2006).

Code de champ modifié

Code de champ modifié

Code de champ modifié

257 Illite/muscovite undergoes a change to mullite and K-feldspar, plus a melt, according to the  
258 following reaction (Elert *et al.*, 2003):



261 In the clays with small amount of carbonates (< 10%), CC1 and CC4 samples, the fired  
262 clays consisted mainly of quartz, diopside, cristobalite, spinel, gehlenite and wollastonite.  
263 Cristobalite appeared in clay with high amount of quartz. We note the absence of the mullite  
264 phase in those samples: small quantities of carbonates (< 10%) clearly inhibit the formation of  
265 mullite and form instead Ca rich aluminosilicates. Mullite was formed in carbonate rich clays  
266 when the carbonates exceed 10%, with sufficient quantity of Al (associated with the  
267 abundance of plagioclase and illite/muscovite). With a small amount of Al, anorthite is  
268 formed instead of mullite.

269 The results can support provenance study issues, in developing a compositional databank  
270 and establishing reference groups of ancient clay from Moroccan sites. Such study could help  
271 to answers some archaeologist's questions concerning places and regions of origin, to  
272 determine technique for the production of artefacts, and to interpret cultural influences.  
273 Therefore, with the determination of the chemical and mineralogical composition of ceramic  
274 shards it will be possible to related it to a specific clays source and conditions of production,  
275 namely the firing temperature.

## 276 CONCLUSION

277 Clay ceramics undergo significant mineralogical modifications upon firing. Different types  
278 of clay-rich materials formed distinct associations of high-temperature phases during firing.  
279 The main assemblage of fired products is controlled by the initial mineralogical composition,  
280 in particular the carbonates content.

Code de champ modifié

281 Firing non-calcareous raw materials produced spinel between 550 and 950°C. Cristobalite  
282 and mullite was formed above 1000°C from clays that contain illite, kaolinite and chlorite. In  
283 clays containing vermiculite and high amount of chlorite, hematite was formed between 550  
284 and 950°C.

285 In calcareous clays, Ca-silicates (diopside, gehlenite and wallostonite) were accompanied  
286 by spinel, cristobalite, mullite, hematite and feldspars. The presence of small amount of  
287 carbonates inhibited mullite formation, and instead Ca-silicates (gehlenite and wallostonite)  
288 were formed. When the carbonates exceeded 10%, mullite was formed, but its formation  
289 depends on the quantity of Al. when the Al content is too low to form mullite, then a small  
290 amount of anorthite is formed instead of mullite.

291 The mineral transformations of natural clays with increasing temperature were studied to  
292 establish reference groups based on raw-material composition and high-temperature  
293 mineralogy. This study should be of interest to the local ceramic industry and should  
294 contribute to a more precise correlation between the composition of ancient ceramic and  
295 potential raw materials in further ancient ceramics studies, namely its provenance.

296

## 297 **REFERENCE**

298 Azarov, G.M., Maiorova, E.V., Oborina, M.A. and Belyakov, A.V. (1995) Wollastonite raw  
299 materials and their applications (a review). *Glass and Ceramics*, **52**, 237-240.

300 Cuevas, J., Leguey, S., Garralón, A., Rastrero, M.R., Procopio, J.R., Sevilla, M.T., Jiménez,  
301 N.S., Abad, R.R. and Garrido, A. (2009) Behavior of kaolinite and illite-based clays as  
302 landfill barriers. *Applied Clay Science*, **42**, 497-509.

303 Cultrone, G., Rodriguez-Navarro, C., Sebastian, E., Cazalla, O. and Torre, M.J.D.L. (2001)  
304 Carbonate and silicate phase reactions during ceramic firing. *European Journal of*  
305 *Mineralogy*, **13**, 621-634.

306 Czímerová, A., Bujdák, J. and Dohrmann, R. (2006) Traditional and novel methods for  
307 estimating the layer charge of smectites. *Applied Clay Science*, **34**, 2-13.

308 Demir, I. (2008) Effect of organic residues addition on the technological properties of clay  
309 bricks. *Waste Management*, **28**, 622-627.

310 De Vleeschouwer, F., Renson, V., Claeys, P., Nys, K. and Bindler, R. (2011) Quantitative wd-  
311 xrf calibration for small ceramic samples and their source material. *Geoarchaeology*,  
312 **26**, 440-450.

313 El Ouahabi, M., Daoudi, L., De Vleeschouwer, F., Bindler, R. and Fagel, N. (2014a)  
314 Potentiality of clay raw materials from northern morocco in ceramic industry: Tetouan  
315 and meknes areas. *Journal of Minerals and Materials Characterization and*  
316 *Engineering*, **2**, 145-159.

317 El Ouahabi, M., Daoudi, L. and Fagel, N. (2014b) Preliminary mineralogical and geotechnical  
318 characterization of clays from morocco: Application to ceramic industry. *Clay*  
319 *Minerals*, **49**, 1-17.

320 Elert, K., Cultrone, G., Navarro, C.R. and Pardo, E.S. (2003) Durability of bricks used in the  
321 conservation of historic buildings - influence of composition and microstructure.  
322 *Journal of Cultural Heritage*, **4**, 91-99.

323 Henn, F., Durand, C., Cerepi, A., Brosse, E. and Giuntini, J.C. (2007) Dc conductivity,  
324 cationic exchange capacity, and specific surface area related to chemical composition  
325 of pore lining chlorites. *Journal of Colloid and Interface Science*, **311**, 571-578.

326 Jordán, M.M., Boix, A., Sanfeliu, T. and de la Fuente, C. (1999) Firing transformations of  
327 cretaceous clays used in the manufacturing of ceramic tiles. *Applied Clay Science*, **14**,  
328 225-234.

329 Jordán, M.M., Sanfeliu, T. and de la Fuente, C. (2001) Firing transformations of tertiary clays  
330 used in the manufacturing of ceramic tile bodies. *Applied Clay Science*, **20**, 87-95.

331 Kam, S., Zerbo, L., Bathiebo, J., Soro, J., Naba, S., Wenmenga, U., Traoré, K., Gomina, M.  
332 and Blanchart, P. (2009) Permeability to water of sintered clay ceramics. *Applied Clay*  
333 *Science*, **46**, 351-357.

334 Khalfaoui, A. and Hajjaji, M. (2009) A chloritic-illitic clay from morocco: Temperature-time-  
335 transformation and neoformation. *Applied Clay Science*, **45**, 83-89.

336 Levin, E.M., Robbins, C.R. and McMurdie, H.F. (1964) *Phase diagrams for ceramists*.  
337 Columbus, OH Edition. American ceramic society.

338 Lin, K.-L. (2007) Use of thin film transistor liquid crystal display (tft-lcd) waste glass in the  
339 production of ceramic tiles. *J Hazard Mater*, **148**, 91-97.

340 Murad, E. and Wagner, U. (1998) Clays and clay minerals: The firing process. *Hyperfine*  
341 *Interactions*, **117**, 337-356.

342 Pardo, F., Meseguer, S., Jordán, M.M., Sanfeliu, T. and González, I. (2011) Firing  
343 transformations of chilean clays for the manufacture of ceramic tile bodies. *Applied*  
344 *Clay Science*, **51**, 147-150.

345 Peters, T. and Iberg, R. (1978) Mineralogical changes during firing of calcium-rich brick  
346 clays. *Ceramic Bulletin*, **57**, 503-509.

347 Tite, M.S. and Maniatis, Y. (1975) Examination of ancient pottery using the scanning electron  
348 microscope. *Nature*, **257**, 122-123.

349 Trindade, M.J., Dias, M.I., Coroado, J. and Rocha, F. (2009) Mineralogical transformations of  
350 calcareous rich clays with firing: A comparative study between calcite and dolomite  
351 rich clays from algarve, portugal. *Applied Clay Science*, **42**, 345-355.

352 Whitney, D. L. and B. W. Evans (2010) Abbreviations for names of rock-forming minerals.  
353 *American Mineralogist*, **95**. 185-187.

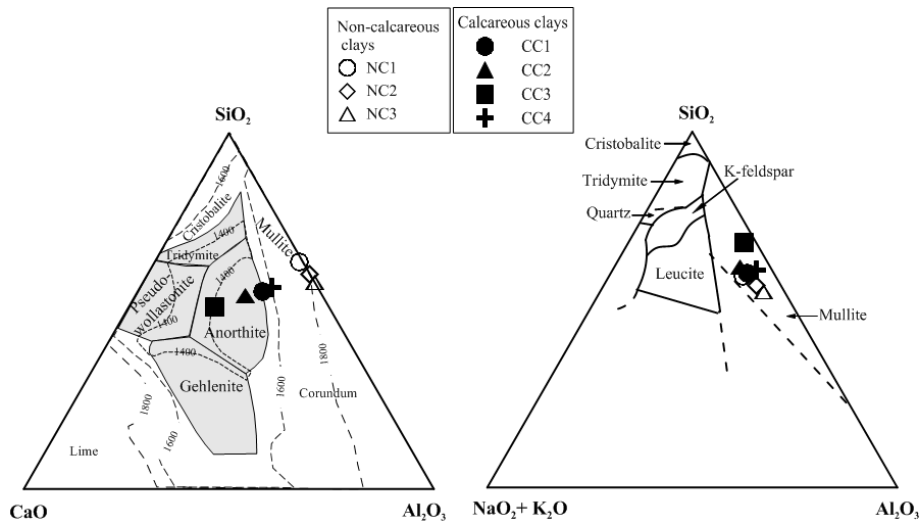
354

355

356 **Figure captions**

357 **Figure 1.** SiO<sub>2</sub>/Al<sub>2</sub>O<sub>3</sub>/CaO and SiO<sub>2</sub>/Al<sub>2</sub>O<sub>3</sub>/NaO<sub>2</sub>+K<sub>2</sub>O equilibrium diagrams (Levin *et al.*,  
358 1964).

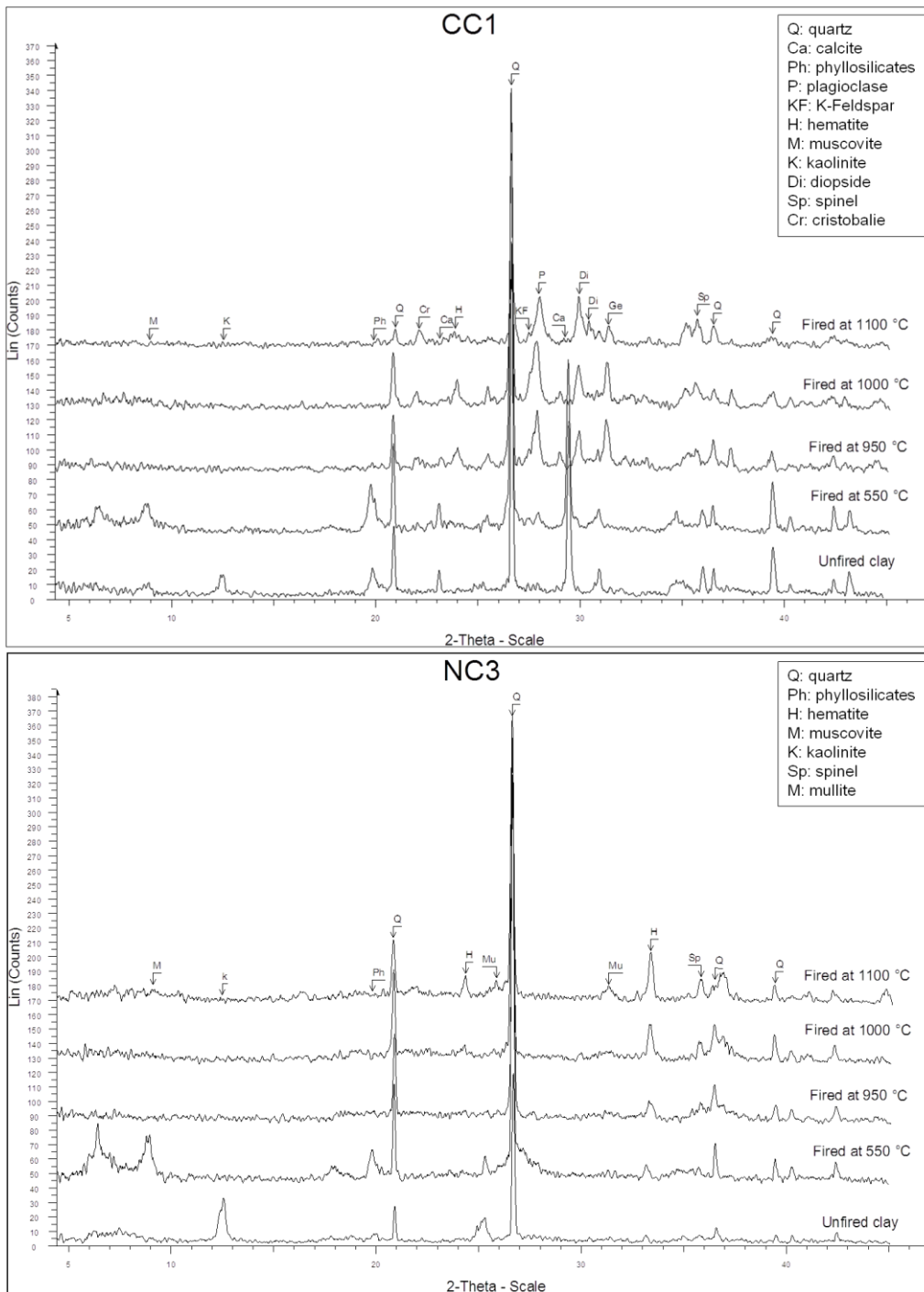
Code de champ modifié



359  
360  
361  
362  
363  
364  
365  
366  
367  
368  
369  
370  
371

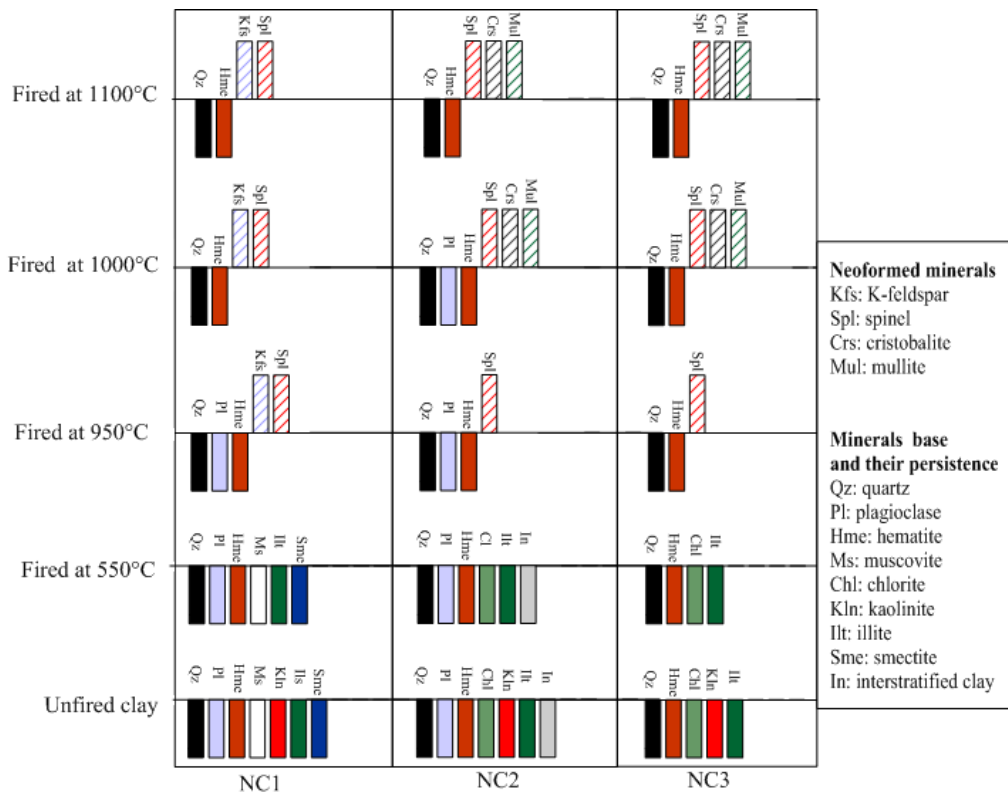


372 **Figure 2.** Example of X-ray powder diffraction patterns of calcareous (CC1) and non-  
 373 calcareous clays (NC3) at different heating temperature.

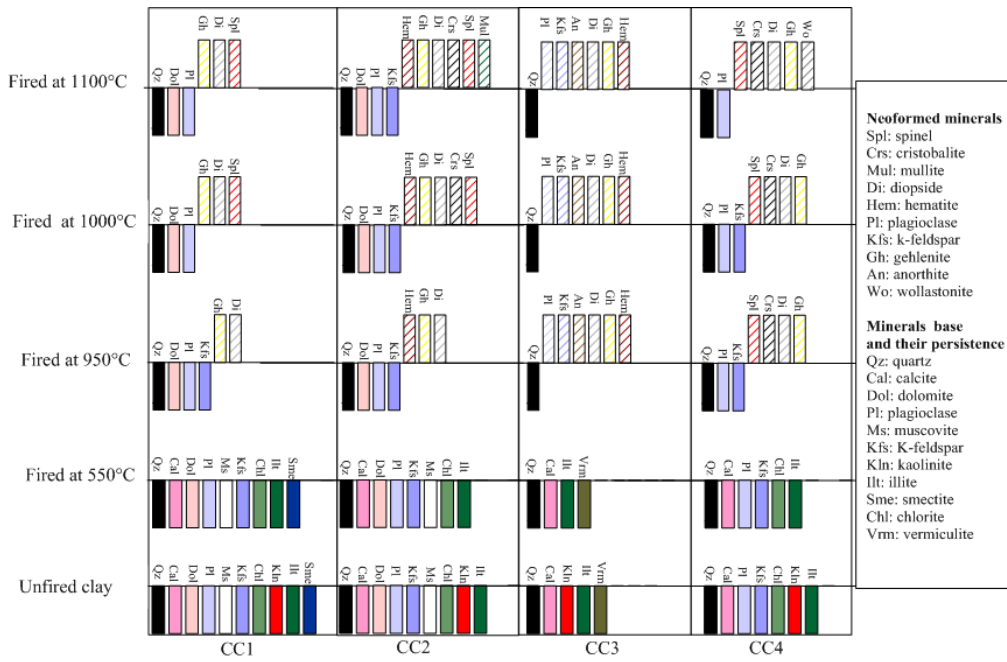


374

375 **Figure 3.** Mineralogical transformations of non-calcareous (a) or calcareous clays (b) during  
 376 firing.



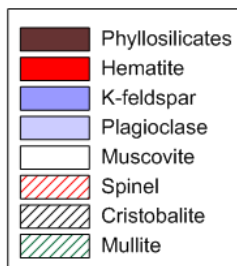
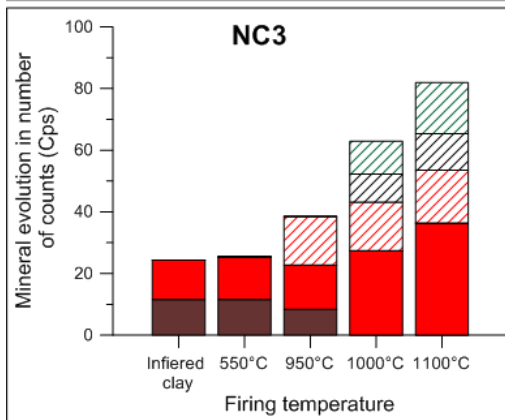
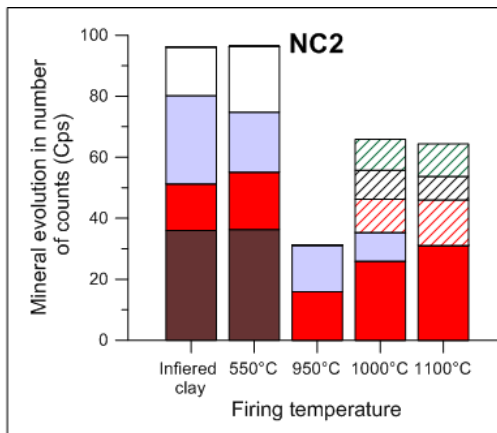
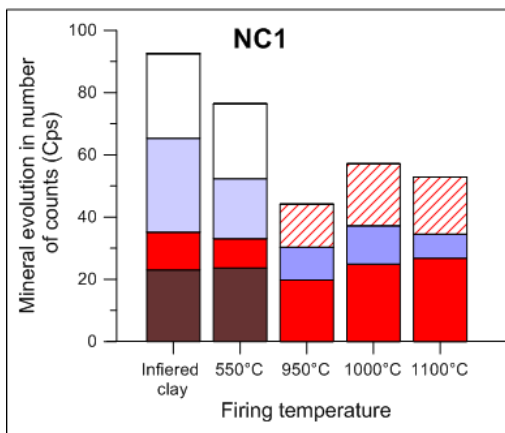
377



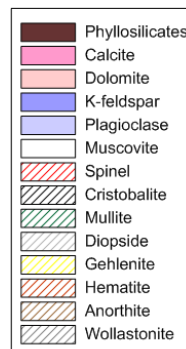
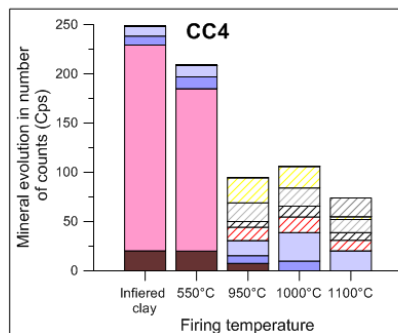
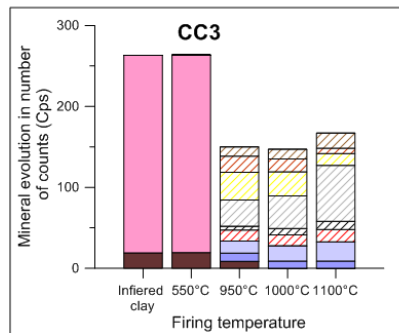
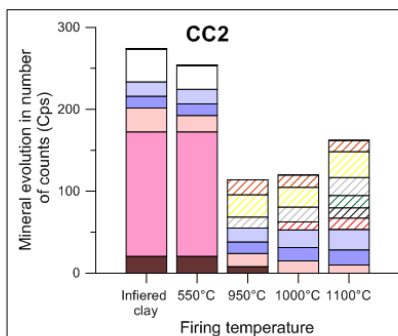
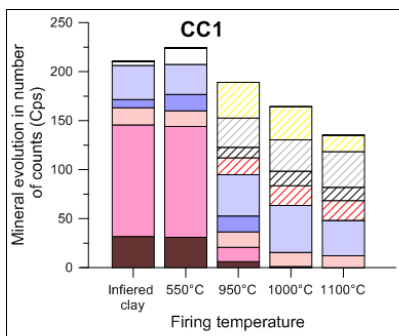
378

379

380 **Figure 4.** Evolution of raw and neoformed mineral contents from non-calcareous (a) or  
 381 calcareous clays (b) with temperature.

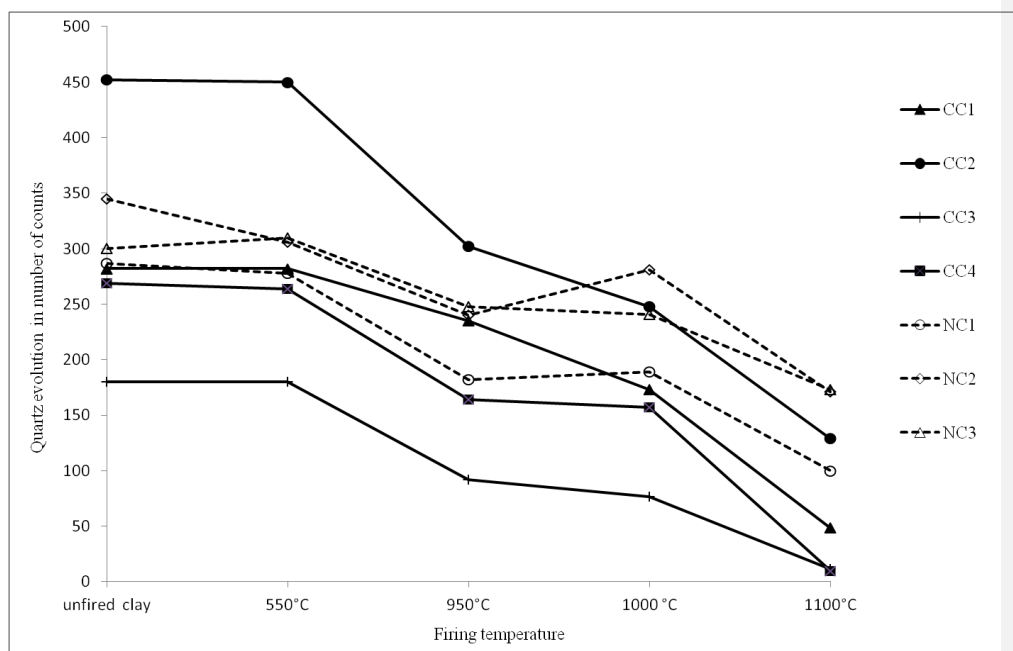


382



383

384 **Figure 5.** Quartz evolution in calcareous and non-calcareous clays according to temperature  
 385 evolution, in number of counts (cps).



386

387

388 **Table captions**

389 **Table 1.** Chemical composition (wt.%) of the studied raw clay. Data from (El Ouahabi *et al.*,  
 390 2014a).

	SiO <sub>2</sub>	Al <sub>2</sub> O <sub>3</sub>	Fe <sub>2</sub> O <sub>3</sub>	CaO	MnO	MgO	Na <sub>2</sub> O	K <sub>2</sub> O	TiO <sub>2</sub>	P <sub>2</sub> O <sub>5</sub>	SO <sub>2</sub>	Total	L.O.Ia
	(%)	(%)	(%)	(%)	(%)	(%)	(%)	(%)	(%)	(%)	(%)	(%)	(%)
NC1	48.2	26.6	15.6	0.6	0.1	2.2	1.3	5.0	0.7	0.2	0.0	100	9.1
NC2	51.5	33.8	0.5	0.0	1.8	1.9	4.4	1.0	0.2	0.1	6.6	100	6.6
NC3	47.6	34.5	0.4	0.0	2.4	1.1	3.3	1.0	0.1	0.0	9.0	99.4	9.0
CC1	44.9	24.8	5.1	11.4	0.1	2.7	0.8	4.1	0.8	0.3	0.2	95.2	17.8
CC2	41.2	20.4	8.3	14.4	0.1	2.8	0.8	4.2	0.7	0.4	0.0	93.3	16.6
CC3	35.4	14.6	12.5	19.2	0.1	0.9	0.2	1.3	0.5	0.5	0.0	85.2	22.6
CC4	45.9	26.2	11.1	9.0	0.0	1.4	0.7	2.2	0.8	0.6	0.0	97.9	15.8

391

392 <sup>a</sup>Loss on ignition at 1000 °C.

393

394

395 **Table 2.** List of mineral abbreviations used in this study, their chemical formula, and the  
 396 diagnostic XRD peaks d(001) values) used for their identification (Whitney and Bernard,  
 397 2010).

Mineral	Abbreviation	Chemical formula	d value for (001) peak
Original minerals			
Quartz	Qz	SiO <sub>2</sub>	3.34
Calcite	Cal	CaCO <sub>3</sub>	3.04
Dolomite	Dol	CaMg(CO <sub>3</sub> ) <sub>2</sub>	2.89
Kaolinite	Kln	Al <sub>2</sub> Si <sub>2</sub> O <sub>5</sub> (OH) <sub>4</sub>	7.18
Muscovite	Ms	KAl <sub>2</sub> [(OH) <sub>2</sub> AlSi <sub>3</sub> O <sub>10</sub> ]	10.0
Clay minerals	Cl	<sup>a</sup> (AlSi <sub>2</sub> O <sub>5</sub> <sup>2-</sup> ) <sub>n</sub>	4.48
Original and neoformed minerals			
K-feldspar	Kfs	(K,Na)AlSi <sub>3</sub> O <sub>8</sub>	3.25
Hematite	Hem	Fe <sub>2</sub> O <sub>3</sub>	2.69
Plagioclase	Pl	(Na,Ca)(Si,Al) <sub>4</sub> O <sub>8</sub>	3.19
Neoformed minerals			
Cristobalite	Crs	SiO <sub>2</sub>	4.05
Gehlenite	Gh	<sup>a</sup> Ca <sub>2</sub> Al <sub>2</sub> SiO <sub>7</sub>	2.85
Mullite	Mul	Al <sub>6</sub> Si <sub>2</sub> O <sub>13</sub>	3.40
Spinel	Spl	MgAl <sub>2</sub> O <sub>4</sub>	2.42
Wollastonite	Wo	CaSiO <sub>3</sub>	3.31
Diopside	Di	CaMgSi <sub>2</sub> O <sub>6</sub>	2.99
Anorthite	An	CaAl <sub>2</sub> Si <sub>2</sub> O <sub>8</sub>	3.20

398 <sup>a</sup> simplified formula

399

400